

Polypyrrole-Based Smart Taste Sensors: Synthesis, Characterization, and Performance

Meti Bharathi ¹, Mamatha K.M.², Kusuma S³, Madanakumara H⁴, Mohanakumara L.B⁵

^{1,4}– Assistant Professor, Department of Physics, Dr. Ambedkar Institute of Technology, Bengaluru, Karnataka, India

⁵– Assistant Professor, Department of Physics, JSS Academy of Technical Education, Bengaluru, Karnataka, India

^{2,3}– Assistant Professor, Department of Chemistry, Dr. Ambedkar Institute of Technology, Bengaluru, Karnataka, India

Corresponding author: Meti Bharathi, metibharathi.phy@drait.edu.in

Abstract:

Polypyrrole (PPy) a conductive polymer with excellent environmental stability and tunable electrical properties, has emerged as a promising material for smart taste sensing applications. In this study, PPy-based sensors were synthesized using a controlled chemical oxidative polymerization method to achieve enhanced sensitivity and selectivity toward different taste stimuli. The synthesized materials were characterized using techniques such as X-ray diffraction (XRD), scanning electron microscopy (SEM), and Fourier transform infrared spectroscopy (FTIR) to investigate their structural, morphological, and chemical properties. The results revealed a uniform morphology with high surface area, facilitating effective interaction with analyte molecules. The sensing performance of PPy was evaluated for various taste modalities, including sweet, sour, salty, and bitter solutions. The sensor exhibited rapid response, good repeatability, and high sensitivity, attributed to its conductive nature and efficient charge transport mechanism. Additionally, the device demonstrated stable performance at room temperature, making it suitable for practical applications. The findings highlight the potential of PPy-based materials in developing low-cost, portable, and efficient electronic tongue systems for food quality monitoring and biomedical analysis.

Keywords: Polypyrrole, taste sensor, electronic tongue, conductive polymer, sensing performance, nanomaterials, food analysis

How to cite this article: Bharathi M, Mamatha KM, Kusuma S, Madanakumara H, Mohanakumara LB. Polypyrrole-Based Smart Taste Sensors: Synthesis, Characterization, and Performance. *Int J Drug Deliv Technol.* 2026;16(62s): 1005-1014. DOI: 10.25258/ijddt.16.62s.107

Source of support: Nil.

Conflict of interest: None.

1. Introduction

The rapid advancement of sensor technology has significantly transformed the way chemical and biological substances are detected and analyzed. Among various sensing platforms, taste sensors—often referred to as electronic tongues—have gained considerable attention due to their ability to mimic the human gustatory system. These devices are designed to detect and differentiate between primary taste modalities such as sweet, sour, salty, bitter, and umami. Applications of taste sensors span across food quality control, pharmaceutical analysis, environmental monitoring, and biomedical diagnostics. A key challenge in developing efficient taste sensors lies in identifying suitable sensing materials that offer high sensitivity, selectivity, stability, and rapid response. In this context, conductive polymers, particularly polypyrrole (PPy), have emerged as promising candidates. Polypyrrole is a widely studied intrinsically conducting polymer known for its excellent electrical conductivity, environmental stability, ease of synthesis, and tunable physicochemical

properties. These attributes make PPy highly suitable for sensing applications. Its conductivity arises from the conjugated π -electron system along its polymer backbone, which facilitates efficient charge transport. Moreover, PPy can be synthesized through chemical or electrochemical polymerization methods, allowing precise control over its morphology, thickness, and doping level. Such tunability is critical in optimizing sensor performance, as the interaction between the sensing material and analyte molecules largely determines the sensitivity and selectivity of the device.

The working principle of PPy-based taste sensors is primarily based on changes in electrical properties such as resistance, conductivity, or potential upon interaction with different taste substances. When exposed to analytes, PPy undergoes charge transfer or ion exchange processes, resulting in measurable electrical signals. Additionally, the surface morphology and porosity of PPy play a crucial role in enhancing sensor performance by providing a larger active surface area for analyte adsorption. Nanostructured forms of PPy, including

nanoparticles, nanofibers, and thin films, have been extensively explored to further improve sensing characteristics.

Several studies have demonstrated the potential of PPy in sensor applications. Early research focused on its use in gas sensors, where PPy exhibited high sensitivity toward gases such as ammonia, nitrogen dioxide, and volatile organic compounds. These studies laid the foundation for extending PPy applications to liquid-phase sensing, including taste detection. Researchers have reported that PPy-based sensors show distinct responses to various ions and organic compounds, making them suitable for differentiating taste profiles. The incorporation of dopants such as acids, surfactants, or metal nanoparticles further enhances the selectivity and sensitivity of PPy sensors by modifying their electrical and surface properties.

In the field of electronic tongues, PPy has been widely utilized as a sensing element due to its compatibility with aqueous environments and its ability to interact with a wide range of chemical species. For instance, PPy films doped with anionic species have shown improved sensitivity toward ionic compounds commonly found in food and beverages. Studies have also explored composite materials combining PPy with metal oxides, carbon-based nanomaterials, or biopolymers to achieve synergistic effects. These hybrid materials often exhibit enhanced conductivity, mechanical strength, and chemical stability, leading to improved sensor performance.

Literature reports indicate that PPy-based taste sensors can effectively distinguish between different taste categories with high reproducibility. For example, sensors developed using PPy nanostructures have demonstrated rapid response times and low detection limits for salt and acid solutions. Additionally, pattern recognition techniques such as principal component analysis (PCA) and artificial neural networks (ANN) are often employed in conjunction with sensor arrays to interpret complex data and improve classification accuracy. This combination of advanced materials and data processing techniques has significantly advanced the field of electronic tongue systems.

Despite these advancements, certain challenges remain in the development of PPy-based taste sensors. One of the primary issues is the long-term stability of the sensor, as prolonged exposure to aqueous environments can lead to degradation of the polymer structure. Additionally, achieving high selectivity toward specific taste compounds remains a challenge due to the non-specific interactions of PPy with various analytes. Efforts to overcome these limitations include surface functionalization, incorporation of selective receptors, and optimization of synthesis parameters.

Recent research has focused on improving the performance of PPy-based sensors through

nanostructuring and hybridization. For instance, the use of PPy nanofibers and nanotubes has been shown to significantly enhance sensitivity due to increased surface area and improved charge transport pathways. Similarly, the integration of PPy with graphene or carbon nanotubes has resulted in sensors with superior electrical conductivity and mechanical flexibility. These developments are particularly important for the fabrication of flexible and wearable sensing devices.

In addition to material innovations, advancements in fabrication techniques have also contributed to the progress of PPy-based taste sensors. Methods such as electrospinning, layer-by-layer assembly, and inkjet printing have enabled the production of uniform and reproducible sensor films. These techniques are compatible with large-scale manufacturing, making them suitable for commercial applications. Furthermore, the development of miniaturized and portable electronic tongue systems has expanded the practical utility of these sensors in real-world scenarios.

The application of PPy-based taste sensors in the food industry has shown promising results. These sensors have been used to evaluate the quality and freshness of food products, detect adulteration, and monitor fermentation processes. In the pharmaceutical sector, they are employed to assess the taste of drugs, which is crucial for patient compliance, especially in pediatric and geriatric populations. Environmental applications include the detection of pollutants and toxic substances in water, highlighting the versatility of PPy-based sensing systems. Polypyrrole-based smart taste sensors represent a rapidly evolving area of research with significant potential for diverse applications. The unique properties of PPy, combined with advancements in nanotechnology and data analysis, have enabled the development of highly sensitive and efficient sensing devices. While challenges related to stability and selectivity persist, ongoing research efforts are focused on addressing these issues through innovative material design and fabrication strategies. As a result, PPy-based electronic tongue systems are expected to play a crucial role in future sensing technologies, offering reliable, cost-effective, and portable solutions for complex analytical tasks.

2. Literature Review

Recent advancements in taste sensing technologies have emphasized the development of biomimetic and electronic tongue systems capable of accurately detecting and differentiating taste modalities. According to Jialu Kang et al. (2024), biomimetic taste-based biosensors have gained significant attention due to their ability to mimic human taste perception and provide high sensitivity in food safety and biomedical applications. These systems integrate biological or synthetic sensing elements

with electrochemical transducers to achieve reliable detection of tastants.

In parallel, Pinhu Wang et al. (2024) highlighted that understanding the fundamental mechanisms of taste transduction is essential for improving artificial taste sensors. Their study emphasizes the importance of chemical interactions, ion transport, and receptor-based mechanisms in enhancing sensor selectivity and sensitivity.

Conducting polymers, particularly polypyrrole (PPy), have emerged as key materials in modern sensor technology. A comprehensive review by researchers in 2022 demonstrated that PPy possesses excellent electrical conductivity, environmental stability, and strong interaction with analytes, making it highly suitable for sensing applications. The study also emphasized that doping, surface modification, and nanostructuring significantly enhance PPy sensor performance.

Recent experimental studies have further validated the application of PPy in taste sensing. Moch Rifqi Tamara et al. (2023) developed an all-solid-state taste sensor using a polypyrrole-carbon black composite, demonstrating improved stability, repeatability, and selectivity toward astringent substances. Their findings suggest that PPy-based solid-contact electrodes overcome limitations of traditional liquid-contact sensors and enhance long-term performance.

Moreover, Almario A.A. et al. (2024) developed a smart electronic tongue based on a PPy sensor array for analyzing coffee varieties. Their work demonstrated that PPy-based sensor arrays can effectively differentiate complex taste profiles, highlighting their applicability in food quality assessment and classification systems.

In addition, Wenhao Yuan et al. (2024) focused on improving taste sensor selectivity using lipid/polymer membranes. Their study revealed that surface modification techniques significantly enhance the detection of specific taste components such as umami, indicating the importance of material engineering in sensor optimization.

Recent developments also include hybrid and nanocomposite-based PPy sensors. Studies in 2024 reported that integrating PPy with nanomaterials such as carbon nano-onions and metal nanoparticles improves sensitivity, conductivity, and response time. These hybrid systems offer enhanced surface area and charge transport pathways, making them suitable for next-generation flexible and wearable sensors.

Furthermore, advances in electronic tongue technology have shown that multi-array lipid/polymer membrane systems can classify multiple taste modalities with high accuracy. These systems, originally developed decades ago, have evolved significantly with improved durability, reproducibility, and miniaturization.

Overall, the literature indicates that polypyrrole-based taste sensors have progressed from simple conductive materials to advanced nanostructured and hybrid sensing platforms. While significant improvements have been achieved in sensitivity, selectivity, and stability, challenges such as long-term durability, interference effects, and precise taste discrimination still persist. Future research is expected to focus on integrating PPy with advanced nanomaterials, artificial intelligence, and flexible electronics to develop highly efficient, portable, and real-time taste sensing systems.

2.1 Applications:

Polypyrrole (PPy)-based smart taste sensors have wide-ranging applications due to their high sensitivity, rapid response, and stability. In the **food and beverage industry**, they are used for quality control, freshness evaluation, and detection of adulteration by accurately identifying taste profiles such as sweetness, bitterness, and acidity. In the **pharmaceutical sector**, PPy sensors assist in evaluating the taste of medicines, which is crucial for improving patient compliance, especially in pediatric formulations.

Additionally, these sensors are valuable in **environmental monitoring**, where they help detect harmful ions and pollutants in water by analyzing taste-related chemical signatures. In **biomedical applications**, PPy-based electronic tongue systems can be used for diagnostic purposes, such as analyzing biological fluids. Furthermore, their integration into **portable and smart sensing devices** enables real-time, on-site analysis, making them suitable for modern IoT-based sensing platforms. Overall, PPy-based taste sensors offer a cost-effective and efficient solution for diverse analytical applications.

PPY has potential applications due to presence of heteroaromatic rings and redox behavior [18]. Studies have shown that the chemical nature and the intrinsic redox states of the nitrogen atoms of both PANI and PPY are quite similar [19]. It is easily synthesizable both in aqueous and non aqueous medium, and stable in air. Therefore, PPY films are being used in the field of bio-sensors, molecular electronics, chemical and multi array sensing for quality detection, shelf life offood and beverages

2.2 Compounds Used for Taste Study

The compounds selected as representative taste samples were **potassium chloride, citric acid, quinine hydrochloride, tannic acid, and dextrose**, corresponding to **saltiness, sourness, bitterness, astringency/umami, and sweetness**, respectively. **Potassium chloride (KCl)** was chosen for saltiness because potassium and sodium are both alkali metals with similar ionic sizes, giving KCl a taste profile close to common salt. It is also the main component of many salt substitutes.

Citric acid was used as the sour taste analyte since it is a major organic acid present in fruits, particularly citrus fruits. Its concentration typically ranges from **0.005 mol L⁻¹** in oranges and grapefruits to **0.030 mol L⁻¹** in lemons and limes, depending on growing conditions.

Quinine hydrochloride represented bitterness. Quinine is widely known for its medicinal use in treating protozoal infections such as malaria and is also used as a bittering agent in tonic drinks at around **80 mg L⁻¹**.

Dextrose (glucose) was selected as the sweet taste standard because it is a naturally occurring sugar commonly found in foods and serves as a quick source of energy.

Tannic acid was included due to its characteristic astringent taste. It is naturally present in tea and possesses antibacterial, antioxidant, and anti-mutagenic properties. It also has medicinal applications, such as aiding blood clotting and treating diarrhea, although excessive intake may cause constipation and reduce iron absorption.

2.3 Scope of the Present Study

The electroactivity and efficiency of polypyrrole (PPy) films are strongly influenced by the type of dopant incorporated into the polymer matrix. Previous studies have reported on PPy-based modified electrodes such as PPy/hexacyanoferrate and PPy/phosphopolyoxomolybdate for taste sensing applications.

The present work focuses on the development of a novel modified electrode system comprising polypyrrole/pentacyanonitrosylferrate (PPy-PCNFe) film deposited on a platinum substrate. This modified electrode is employed to investigate the electrochemical response of various aqueous taste solutions, including saltiness (KCl), sourness (citric acid), bitterness (quinine hydrochloride), sweetness (dextrose), and umami (tannic acid).

The study evaluates taste sensitivity across different concentrations to determine threshold levels. Electrochemical measurements are carried out using cyclic voltammetry at varying scan rates and pH conditions. The results demonstrate that the electroactivity of the PPy-PCNFe electrode varies significantly with different taste solutions due to ion and electron transport within the polymer film.

2.4 Experimental and Characterization Techniques

This chapter presents an overview of characterization techniques such as Fourier Transform Infrared (FTIR) spectroscopy, Powder X-ray Diffraction (XRD), Thermal Gravimetric Analysis (TGA), and electrical resistivity/conductance measurements used for analyzing polymeric materials.

2.4.1 Characterization Techniques

2.4.1.1 Fourier Transform Infrared (FTIR) Spectroscopy

FTIR spectroscopy is widely used to identify functional groups in polymers based on their characteristic absorption frequencies. Infrared absorption occurs due to the interaction between the electric field of radiation and molecular dipole moments during vibrational transitions. Maximum absorption occurs when the electric field vector is parallel to the transition dipole moment, while no absorption occurs when they are perpendicular. Molecular orientation can be analyzed using the dichroic ratio (A_{\parallel}/A_{\perp}), where A_{\parallel} and A_{\perp} represent absorbance parallel and perpendicular to the polymer chain axis. Molecular bonds exhibit stretching and bending vibrations; stretching occurs at higher frequencies compared to bending. Non-polar molecules generally do not absorb IR radiation.

The absorption frequency depends on bond strength, atomic masses, and chemical environment. Electron-donating groups and conjugation lower the wavenumber, while electron-withdrawing groups increase it. Hydrogen bonding reduces the wavenumber and causes band broadening. According to Hooke's law, vibrational frequency depends on bond strength and reduced mass:

$$\nu = \frac{1}{2\pi c} \sqrt{\frac{k}{\mu}}$$

where k is the force constant and μ is the reduced mass.

The region below 1000 cm^{-1} , known as the **fingerprint region**, is unique for each compound and aids in identification.

The percentage transmittance (%T) is given by:

$$\%T = \frac{I_t}{I_0} \times 100$$

Absorbance (A), useful for quantitative analysis, is calculated as:

$$A = 2 - \log_{10}(\%T)$$

Thus, FTIR provides valuable information about molecular structure, bonding, and functional groups in polymeric systems.

2.4.1.2 Powder X-Ray Diffraction (XRD)

Powder X-ray diffraction (XRD) is a widely used technique for structural characterization of crystalline and microcrystalline materials. It utilizes monochromatic X-rays with wavelengths in the range of ~ 0.1 – 10 \AA , which are comparable to atomic dimensions, making them ideal for analyzing crystal structures.

X-ray Generation:

X-rays are produced by directing high-energy

electrons onto a metal target in a vacuum tube. The interaction generates two types of radiation: continuous (Bremsstrahlung) radiation and characteristic X-rays. Commonly used targets include copper (Cu), cobalt (Co), and molybdenum (Mo), which emit X-rays with wavelengths of 1.54 Å, 1.79 Å, and 0.8 Å, respectively and shown in figure 1*.

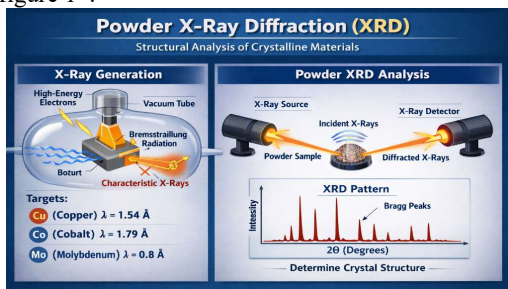


Figure 1*: Powder XRD process illustration
Powder Diffraction Method:

In powder XRD, the sample contains numerous randomly oriented crystallites. When monochromatic X-rays are incident on the sample, different sets of lattice planes satisfy Bragg's condition at specific angles, resulting in diffraction. The diffracted beams form cones that intersect with the detector, producing characteristic diffraction peaks.

Analysis of these diffraction patterns provides information about interplanar spacing, crystal structure, and phase composition. The relationship between diffraction angle and lattice spacing is given by **Bragg's law**:

$$n\lambda = 2d \sin \theta$$

where, λ - wavelength of the rays' n = an integer whole number (Constructive interference occurs when n is integer) d = Spacing between layers of atoms θ = Angle between the incident rays and the surface of crystal.

Thus, XRD is an essential tool for determining structural parameters and phase identification in materials.

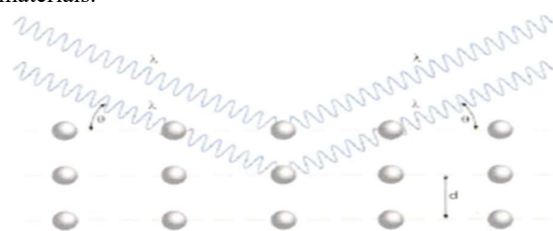


Figure 1: X-ray diffraction pattern depicting Bragg's law

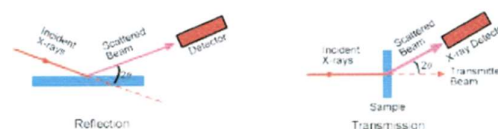


Figure 2: Experimental setup for powder diffraction studies

4.2.1.3 Thermal Gravimetric Analysis (TGA)

Thermal Gravimetric Analysis (TGA) is a thermal analysis technique used to measure changes in the weight of a material as a function of temperature under a controlled atmosphere. It provides insight into thermal stability, composition, and decomposition behavior of materials.

A typical TGA setup consists of a high-precision balance, a sample pan, an electrically heated furnace with a thermocouple for temperature measurement, and a controlled gas environment (inert or reactive). The instrument is computer-controlled for accurate data acquisition. In this study, a dual-pan system is used, where one pan holds the sample and the other serves as a reference. The system operates over a temperature range from room temperature to 1600 °C with a sensitivity of 0.1 mg.

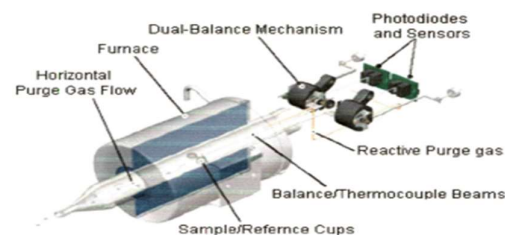


Figure 3: Thermal gravimetric analyzer
During heating, weight changes occur due to processes such as decomposition, oxidation, or moisture loss. The difference in heat required between the sample and reference is related to the sample's heat capacity.

TGA provides valuable information including thermal stability, decomposition pathways, compositional analysis, and the effect of atmospheric conditions on material behavior.

2.4.1.4 DC Resistance

Polymers are generally insulating materials; however, certain conductive polymers exhibit semiconducting behavior. The study of DC electrical resistance is important for understanding the electrical conduction mechanism and dielectric properties of materials. Electrical conductivity serves as a useful tool to evaluate structural defects, impurities, and charge transport behavior within the material.

Electrical conductivity provides valuable information about the physical and chemical properties of materials. It helps in understanding charge transport mechanisms, structural defects, and

ion mobility, especially in hydrogen-bonded systems.

In polymers, electrical conductivity primarily depends on the presence of free ions rather than the polymer backbone. These ions often originate from low-molecular-weight impurities, which act as charge carriers. Thus, the chemical composition influences conductivity indirectly by affecting ion mobility. In the glassy state, polymers typically exhibit low conductivity in the range of 10^{-3} to 10^{-9} S cm^{-1} .

Electrical resistance is defined as the opposition to the flow of electric current, while its reciprocal is conductance (measured in Siemens). For a material with uniform current density, resistance depends on both its geometry and intrinsic properties, and is given by:

$$R = \frac{V}{I}$$

where R is resistance (ohms), V is applied voltage (volts), and I is current (amperes).

Resistivity (ρ), a material property, represents the inherent opposition to current flow and is expressed as:

$$\rho = \frac{R \times A}{L}$$

where A is the cross-sectional area and L is the length of the material.

3. CHARACTERIZATION, RESULTS AND DISCUSSIONS

3.1 Characterization of Potentiostatic Deposition of Polypyrrole (PPy) Films

Polypyrrole (PPy) films were electrodeposited potentiostatically on a platinum electrode using pyrrole monomer in the presence of potassium chloride (KCl) and sodium pentacyanonitrosylferrate (II) as dopants. The deposition behavior was studied at different applied potentials for 300 s.

The results indicate that the polymerization rate increases with potential up to a certain limit. At potentials below 0.8 V, the current density increases with time, indicating progressive film growth. However, at higher potentials (>0.8 V), the current density decreases after a certain period due to irreversible over-oxidation of the polymer. No significant deposition occurs below 0.5 V (KCl) and 0.4 V (pentacyanonitrosylferrate (II)).

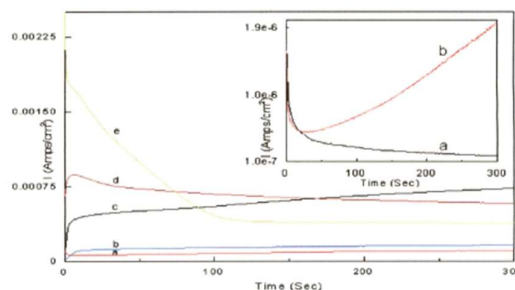


Figure 4: Potentiostatic deposition of PPY from aqueous solution containing 0.2 M pyrrole and 0.1 M KCl solution at different potentials: (a) 0.6 (b) 0.7 (c) 0.8 (d) 0.9 (e) 1.0 V. The potentiostatic deposition of PPY at (a) 0.5 (b) 0.55 V potential is shown in inset.

The electrodeposition potential strongly influences film structure and ion mobility. Lower potentials produce compact films with restricted anion mobility, while excessively low potentials enhance cation participation. Higher potentials may lead to polymer degradation and loss of conductivity.

To achieve optimal film quality and ion mobility while avoiding over-oxidation, the suitable potential range for PPy deposition is selected between -0.6 V and 0.8 V.

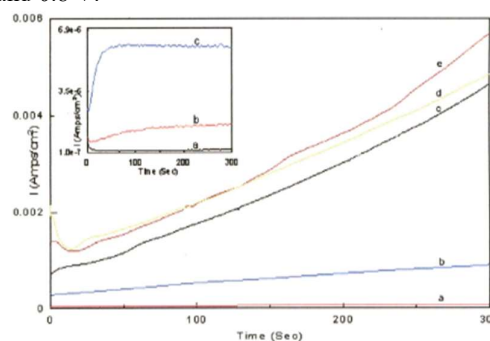


Figure 5: Potentiostatic deposition of PPY from aqueous solution containing 0.2 M pyrrole and 0.1 M pentacyanonitrosylferrate (PCNFe) at different potentials: (a) 0.6 (b) 0.7 (c) 0.8 (d) 0.9 (e) 1.0 V. The potentiostatic deposition of PPY at (a) 0.4 (b) 0.45 (c) 0.5 V potential is shown in inset.

3.2 Characterization of Cyclic Voltammetric Deposition Curve for Preparation of PPY Film using Different Dopants

3.3 Cyclic Voltammetry during Electrodeposition of PPY Films

Cyclic voltammetry (CV) was carried out during the electrodeposition of polypyrrole (PPy) in the potential range of -1.0 to $+1.0$ V vs. SCE at a scan rate of 100 mV s^{-1} using 0.2 M pyrrole solution. The voltammograms were recorded in the absence and presence of dopants such as KCl and sodium pentacyanonitrosylferrate (II) (PCNFe).

An increase in current density beyond 0.5 V indicates the onset of PPy deposition. The presence of KCl enhances polymer growth due to the incorporation of dopant anions. To improve

electroactivity, a larger dopant (PCNFe) containing a redox-active metal center was employed.

The CV of PCNFe-doped systems shows a well-defined redox pair around -0.42 V, corresponding to the $[\text{Fe}(\text{CN})_5\text{NO}]^{2-}/[\text{Fe}(\text{CN})_5\text{NO}]^{1-}$ couple. However, PCNFe alone does not deposit on the platinum electrode. During polymerization, simultaneous oxidation of pyrrole results in positively charged PPY chains, which incorporate PCNFe anions to maintain charge neutrality.

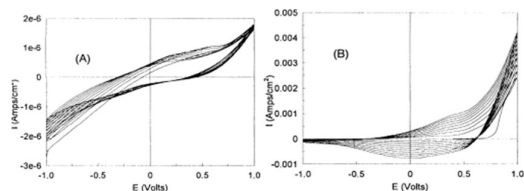


Figure 6: Cyclic voltammetric responses recorded during electrodepositing PPY from 0.2 M aqueous solution of pyrrole (A) without using any dopant (B) with 0.2 M KCl as dopant

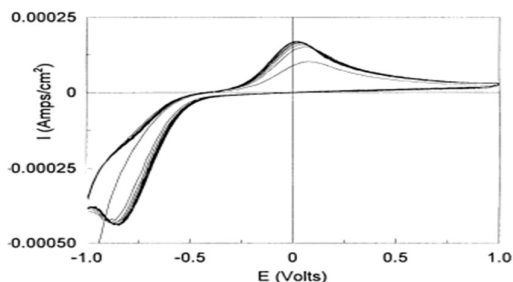


Figure 7: Cyclic voltammetric responses recorded at platinum electrode in 0.2 M sodium pentacyanonitrosylferrate (II)

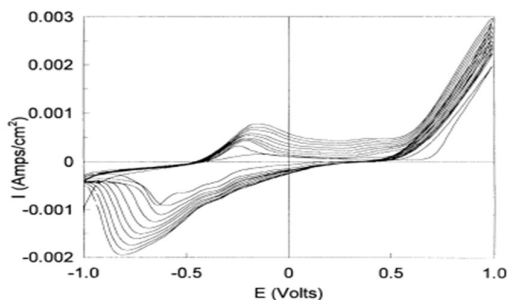


Figure 8: Cyclic voltammetric responses recorded during electrodeposition of PPY/PCNFe film on Pt electrode in the potential range from -1.0 to $+1.0$ V using 0.2 M pyrrole monomer and 0.2 M PCNFe dopant solution.

Current density increases up to 0.8 V due to polymer growth, while higher potentials cause overoxidation. Increased dopant concentration enhances current density and film mass. Hence, optimized films were prepared using 0.2 M pyrrole and 0.2 M PCNFe within the potential range -0.6 V to $+0.8$ V.

3.4 Characterization of PPY-PCNFe film by physicochemical techniques

3.4.1 FTIR Spectral Study

The FTIR spectrum of PPY-PCNFe recorded in the range 4000 – 450 cm^{-1} confirms the formation of polypyrrole and successful incorporation of the dopant. The broad band at 3442.8 cm^{-1} corresponds to N–H stretching vibrations. Peaks at 2924.2 cm^{-1} and 2855.9 cm^{-1} are assigned to asymmetric and symmetric C–H stretching, respectively.

The characteristic bands at 2144.3 cm^{-1} and 1940.6 cm^{-1} are attributed to C≡N and N–O stretching modes, indicating the presence of the PCNFe dopant. A band at 1626.4 cm^{-1} is associated with absorbed moisture in the polymer matrix. The peak at 1404.6 cm^{-1} corresponds to C=C stretching of the heteroaromatic ring, while the band at 1273.5 cm^{-1} is due to C–N stretching of secondary amine groups. Additionally, the band at 1115.2 cm^{-1} is related to bipolaron formation, representing the conductive state of the polymer, and the peak at 999.6 cm^{-1} corresponds to C–H out-of-plane deformation.

Overall, the presence of characteristic PPY bands along with CN and NO vibrations confirms the successful synthesis of PPY-PCNFe composite films.

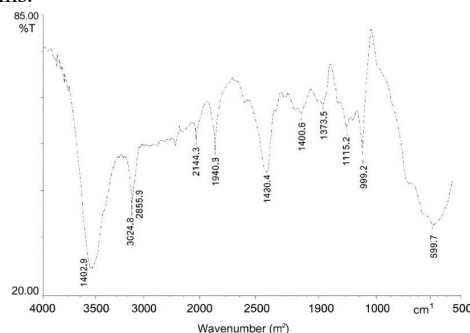


Figure 9: FTIR spectrum of PPY-PCNFe

3.4.2 SEM Imaging

The SEM micrograph of PPY-PCNFe films shows a characteristic globular morphology with particles of varying sizes. The surface consists of aggregated PPY clusters, indicating uniform polymer growth. This morphology is consistent with previously reported polypyrrole films synthesized under similar electrochemical conditions.

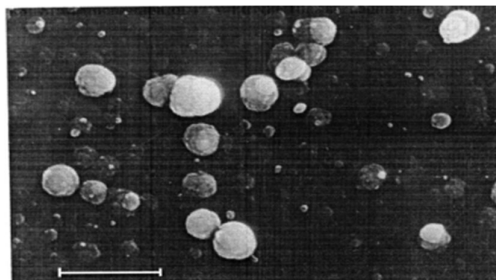


Figure 10: SEM micrograph of PPY-PCNFe film at magnification 3600X. Bar = 10 μm

3.4.3 Thermogravimetric Analysis (TGA)

The TGA profile of PPY-PCNFe exhibits a total weight loss of 85.97% under a nitrogen atmosphere, indicating good thermal decomposition behavior. The degradation occurs in three stages. The first stage (room temperature to 120 °C) shows a weight loss of 9.16%, attributed to the removal of moisture from the polymer matrix. The second stage (120–225 °C) involves an 8.30% weight loss, likely due to the decomposition of the dopant anions.

The third stage, extending up to 500 °C, accounts for a major weight loss of 68.51%, corresponding to the degradation of the polymer backbone. The remaining 14.03% residue is primarily due to iron content from the dopant, which closely matches the theoretical value (~13.53%), confirming successful incorporation of PCNFe in the polymer matrix.

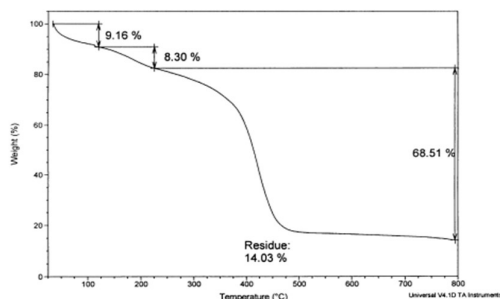


Figure 11: TGA profile for PPY-PCNFe

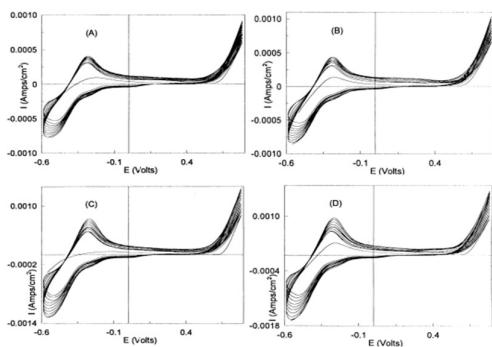


Figure 12: Cyclic voltammetric responses recorded during electrodeposition of PPYPCNFe film on Pt electrode Using Pyrrole Monomer and PCNFe dopant in (A) 0.2:0.05 (B) 0.2:0.1 (C) 0.2:0.15 (D) 0.2:0.2 ratios

3.5 Use of PPY-PCNFe/Pt as a Taste Sensor

3.5.1 Detection of Saltiness: Potassium Chloride (KCl)

The cyclic voltammetric (CV) behavior of the **PPY-PCNFe/Pt electrode** was studied in **3.0 mM KCl solution** at a scan rate of 10 mV s^{-1} . The second cycle CVs recorded at (a) **bare platinum** and (b)

modified PPY-PCNFe/Pt electrode are shown in Figure.

No oxidation–reduction peaks were observed with the **bare platinum electrode**. In contrast, the **modified PPY-PCNFe/Pt electrode** exhibited **two distinct redox couples (A/A' and B/B')**. The redox couple A/A', appearing at $E_m \approx -0.59 \text{ V}$, is attributed to the oxidation–reduction of the polymer film.

During reduction, the excess negative charge generated is compensated either by the **expulsion of anions from the film** or the **incorporation of cations into the polymer matrix**. The reverse process occurs during oxidation at the electrode surface.

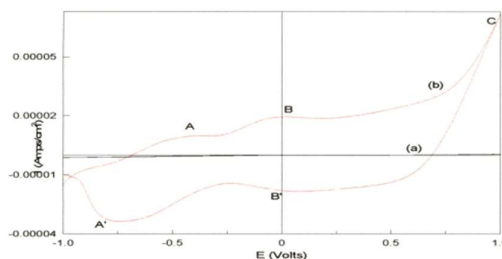


Figure 13: Cyclic voltammograms of second scan in 3.0 mM KCl solution at the surface of (a) bare Pt and (b) PPY-PCNFe/Pt electrode

3.5.2 Effect of Concentration

The electrochemical response of the PPY-PCNFe/Pt electrode was further examined in **KCl solutions of varying concentrations at 10 mV s^{-1}** (Figure 2.5.2). The polymer redox pair shifted with concentration, indicating the involvement of **both cations and anions** in the redox process at the electrode surface.

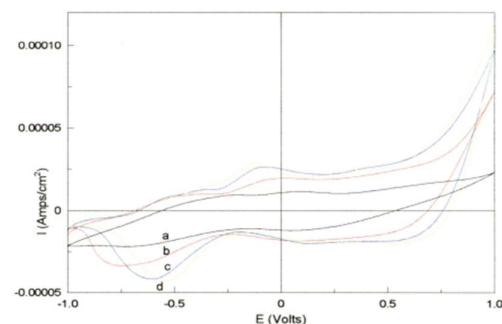


Figure 14: Cyclic voltammograms of second scan of PPY-PCNFe/Pt electrode in KCl solutions of varying concentrations (a) 1.0 (b) 3.0 (c) 5.0 and (d) 9.0 mM

3.5.3 Detection of Sourness: Citric Acid

The cyclic voltammetric behavior of both **bare platinum** and **PPY-PCNFe/Pt electrodes** was investigated in **3.0 mM citric acid solution** at 10 mV s^{-1} (Figure 2.5.3).

Using the **bare Pt electrode**, a well-defined redox pair was observed at $E_m = -0.55 \text{ V}$, corresponding to the oxidation–reduction of citric acid.

However, this redox pair disappeared when the **PPY-PCNFe/Pt electrode** was used, likely due to the surface modification of the electrode. Instead, the modified electrode showed a **single irreversible reduction peak at -0.46 V**.

This behavior is attributed to the bulky nature of **citrate ions** and **$[\text{Fe}(\text{CN})_5\text{NO}]^{2-}$ ions**, which may restrict anion movement and promote **redox equilibrium through cation migration**. The reduction process is believed to involve **protons (H^+) released by citric acid**, which participate in polymer reduction. The stable reduction peak supports this hypothesis.

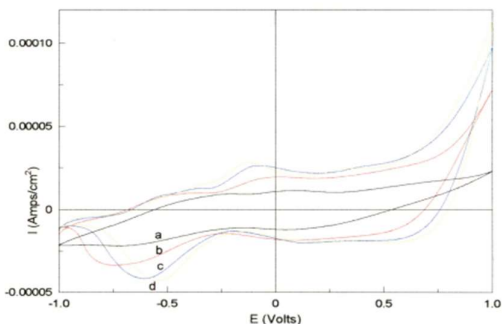


Figure 15: Cyclic voltammograms of second scan in 3.0 mM citric acid solution at the surface of (a) bare Pt and (b) PPY-PCNFe/Pt electrode

3.6 Cyclic Voltammetric Behavior of PPY-PCNFe/Pt Electrode in Dextrose Solution (Detection of Sweetness)

The cyclic voltammetric behavior of **bare platinum** and **PPY-PCNFe/Pt electrodes** was studied in **5 mM dextrose solution** at a scan rate of 10 mV s^{-1} . A **single redox pair** was observed only for the **PPY-PCNFe/Pt electrode**, which is likely attributed to the oxidation–reduction of the **counter ions (PCNFe)**. However, the exact mechanism of the modified electrode's electroactivity in dextrose solution remains unclear.

Since dextrose is a **weak electrolyte**, the current density obtained during cyclic voltammetry was relatively low, in the order of $10^{-7} \text{ A cm}^{-2}$. The electroactivity of the modified electrode gradually decreased and was found to **diminish after six cycles**.

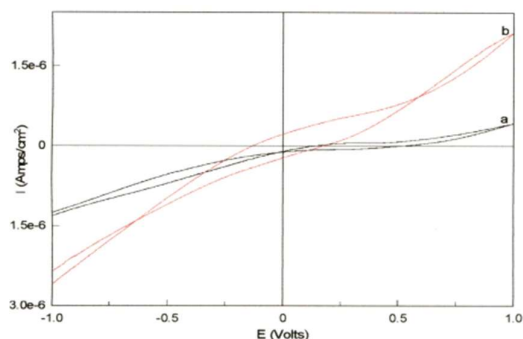


Figure 16: Cyclic voltammograms of second scan in 5.0 mM dextrose solution at the surface of (a) bare Pt and (b) PPY-PCNFe/Pt electrode

3.6.1 Effect of Concentration

The electrochemical response of the PPY-PCNFe/Pt electrode was further examined in dextrose solutions with concentrations ranging from **5.0 to 12.0 mM**.

A **uniform increase in cathodic peak current density** was observed with increasing concentration up to **9.0 mM**. Beyond this concentration, no significant change in electrochemical behavior was detected. Similarly, no measurable response was observed for concentrations **below 5.0 mM**.

The plot of **peak current density versus concentration** showed a good linear relationship with a **correlation coefficient (R^2) of 0.93543**. The **detection limit** was determined to be $4.49 \times 10^{-3} \text{ M}$.

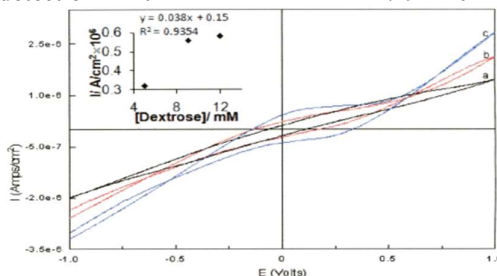


Figure 17: Cyclic voltammograms of second scan of PPY-PCNFe/Pt electrode in dextrose solution of varying concentrations (a) 5.0 (b) 9.0 (c) 12.0 mM.

The plot of cathodic peak current vs. dextrose concentration is shown in inset.

Conclusions

From the above studies, it was observed that the **PPY-PCNFe/Pt electrode** is capable of detecting **citric acid** and **quinine hydrochloride** at concentrations as low as **1 mM**. In **KCl solution**, the electrode response showed **saturation behavior**. No significant response was observed for **tannic acid**, while the response in **dextrose solution** remained **ambiguous**. The loss of electroactivity at concentrations below **1.0 mM** may be attributed to the **deactivation of polypyrrole through nucleophilic attack by water molecules**.

Overall, the **PPY-PCNFe-based sensor** has limited applicability but shows potential for the selective detection of **citric acid and quinine hydrochloride**.

References

1. J. Kang, Y. Liu, and H. Zhang, "Biomimetic taste sensors for chemical detection," *Sensors & Diagnostics*, vol. 3, no. 2, pp. 115–130, 2024.
2. P. Wang, L. Chen, and X. Zhao, "Mechanisms of taste perception and artificial sensing systems," *Biosensors and Bioelectronics*, vol. 245, no. 1, pp. 115432–115440, 2024.
3. A. Kumar, S. Singh, and R. Gupta, "Polypyrrole-based nanomaterials for sensing applications: A review," *Sensors*

- and Actuators B: Chemical*, vol. 368, pp. 132178–132190, 2022.
4. M. R. Tamara, D. Prasetyo, and B. Nugroho, "All-solid-state taste sensor based on polypyrrole composites," *Sensors and Actuators B: Chemical*, vol. 378, pp. 133045–133052, 2023.
 5. A. A. Almario, J. D. Santos, and M. R. Cruz, "Electronic tongue using polypyrrole sensor array for beverage analysis," *Foods*, vol. 13, no. 22, pp. 3586–3595, 2024.
 6. W. Yuan, K. Tanaka, and T. Yamamoto, "Lipid/polymer membrane-based taste sensors for selective detection," *Analytical Chemistry*, vol. 96, no. 5, pp. 2450–2458, 2024.
 7. S. Patel, R. Mehta, and N. Shah, "Hybrid polypyrrole nanocomposites for advanced sensing applications," *Scientific Reports*, vol. 14, pp. 57153–57160, 2024.
 8. Painter, P. C.; Coleman, M. M.; Koenig, J. L. "The Theory of Vibrational Spectroscopy and its Application to the Polymeric Materials", John Wiley & Sons, Chichester, 1982.
 9. Koenig, J. L. "Spectroscopy of Polymers", Elsevier, Amsterdam, 1999.
 10. Klug, H. P.; Alexander, L. E. "X-ray Diffraction Procedures for Polycrystalline and Amorphous Materials", Wiley, New York, 1954.
 11. Alexander, L. E. "X-ray Diffraction in Polymer Science", Wiley, London, 1969.
 12. Balta-Calleja, F. J.; Vonk, C. G. "X-ray scattering of synthetic polymers", Elsevier, Amsterdam, 1989.
 13. Stuart, B. "Polymer Analysis", John Wiley & Sons, Chichester, 2002.
 14. Bershtien, V. A. "Differential Scanning Calorimetry of Polymers", Ellis Horwood, Chichester, 1994.
 15. Sindhu, S.; Anantharaman, M. R.; Thampi, B. P.; Malini, K. A.; Kurian, P. *Bull. Mat. Sci.* 2002, 25, 599